Journal of Experimental Botany, Vol. 64, No. 15, pp. 4681–4695, 2013
doi:10.1093/jxb/ert268 Advance Access publication 7 September, 2013

Journal of Experimental Botany
www.jxb.oxfordjournals.org

REVIEW PAPER

Modes of deformation of walled cells

Jacques Dumais*

Facultad de Ingeniería y Ciencias and Centro de Innovación en Bioingeniería, Universidad Adolfo Ibáñez, Viña del Mar, Chile

* To whom correspondence should be addressed. E-mail: jacques.dumais@uai.cl

Received 8 April 2013; Revised 10 June 2013; Accepted 1 July 2013

Abstract

The bewildering morphological diversity found in cells is one of the starkest illustrations of life's ability to self-organize. Yet the morphogenetic mechanisms that produce the multifarious shapes of cells are still poorly understood. The shared similarities between the walled cells of prokaryotes, many protists, fungi, and plants make these groups particularly appealing to begin investigating how morphological diversity is generated at the cell level. In this review, I attempt a first classification of the different modes of surface deformation used by walled cells. Five modes of deformation were identified: inextensional bending, equi-area shear, elastic stretching, processive intussusception, and chemorheological growth. The two most restrictive modes—inextensional and equi-area deformations—are embodied in the exine of pollen grains and the wall-like pellicle of euglenoids, respectively. For these modes, it is possible to express the deformed geometry of the cell explicitly in terms of the undeformed geometry and other easily observable geometrical parameters. The greatest morphogenetic power is reached with the processive intussusception and chemorheological growth mechanisms that underlie the expansive growth of walled cells. A comparison of these two growth mechanisms suggests a possible way to tackle the complexity behind wall growth.

Key words: Cell mechanics, cell wall, chemorheology, equi-area deformation, *Euglena*, inextensional deformations, intussusception, morphogenesis, pollen grains, prokaryotes, S-layer, tip growth, turgor pressure.

Introduction

Of cellular morphogenesis it can justly be said that we know much but understand little.

Franklin Harold (1990)

If something can be said of the cells that populate even the smallest drop of water, it is that they are morphologically diverse. Cells are also the smallest bits of matter that can be appropriately described as living—thus the multifarious forms of cells is a unique window into the power of organization of life in its purest and simplest form. As we elucidate how cells build themselves from the non-living molecular components within them, we are getting a bit closer to understanding how life can spring and develop from the inorganic world.

Cells occupy a unique length scale that lies just above the reaches of molecular self-assembly; so, although the much smaller (and non-living) viruses can use proteins as literal building blocks to create shapes (Crick and Watson, 1956; Caspar and Klug, 1962), cells have had to make use of other strategies for shape generation where the relationship between the genetic information contained in DNA and the shape of the cell is not so literal as in protein self-assembly. With the exception of perhaps the biconcave geometry of erythrocytes (Sheetz and Singer, 1974; Elgsaeter *et al.*, 1986), none of the morphogenetic strategies used by cells is very well understood. There is certainly abundant information on the molecular controls of morphogenesis, yet the painstaking work of putting the pieces together into compelling morphogenetic models is only beginning. Unfortunately, Franklin Harold's statement is as valid today as it was more than two decades ago.

The broadest class of cells encountered in nature comprises those endowed with a stiff extracellular matrix—the so-called *walled cells*. Extracellular polymeric walls are the norm in prokaryotes, many protists, fungi and plants. Walled cells

distinguish themselves from other cells in that their shape is maintained by their surface. Although internal structures such as the various components of the cytoskeleton play a critical role in controlling the morphogenesis of walled cells, they do not directly maintain cell shape. Accordingly, most walled cells keep their shape even when the entire cytoplasmic content has been removed, leaving behind a perfectly formed wall ghost. Besides the most common polysaccharide-based cell walls, special cases are represented by the protein-based pellicle of euglenoid algae (Suzaki and Williamson, 1985, 1986) and the crystalline surface layers found in prokaryotes (Houwink, 1956; Pum *et al.*, 1991) and certain Volvocales algae (Roberts *et al.*, 1985; Woessner and Goodenough, 1994). Although structurally distinct from the polysaccharide walls, the cortical pellicle and surface layers are mechanically similar to the classical walls in that cell shape is defined by the properties of a stiff layer located directly below or above the plasma membrane. The shared similarities between the walled cells broadly defined make this group particularly appealing to begin investigating how morphological diversity is generated at the cell level.

A few investigators have attempted to identify different strategies of walled-cell morphogenesis based on kinematics (Green *et al.*, 1970; Geitmann and Ortega, 2009). These classifications distinguish, for example, between the well-known cases of diffuse growth and tip growth. However, the limits of a classification based on geometrical attributes have also been noted. At the level of the cell, Green (1969) emphasized that the same final morphology can be achieved via many surface deformation pathways (Fig. 1A). Therefore, an observed shape change is not sufficient to specify the mechanism of wall deformation. Even the deformation of a small wall element may have alternative explanations that cannot be inferred from geometry alone. For example, anisotropic wall expansion can emerge from isotropic stresses acting on a mechanically anisotropic cell wall or from anisotropic stresses acting on a mechanically isotropic wall (Fig. 1B) (Dumais *et al.*, 2004). In terms of cellular control, these two alternatives have very distinct implications that would be missed if attention were paid only to the kinematics rather than the details of the deformation mechanism at the microstructural level. In other words, a strict focus on wall kinematics is often problematic if our goal is to arrive at an understanding of the mechanism of wall deformation.

Here, I adopt a classification of cell morphogenesis using the mechanism of wall deformation as the central criterion. In this context, diffuse growth and tip growth emerge as two related morphogenetic strategies within the rich universe of wall-deformation mechanisms. The diversity of walled cells is such that the list provided is likely to be incomplete. Yet, it seems that even a tentative classification can play an important role in organizing the field and highlighting important areas of research.

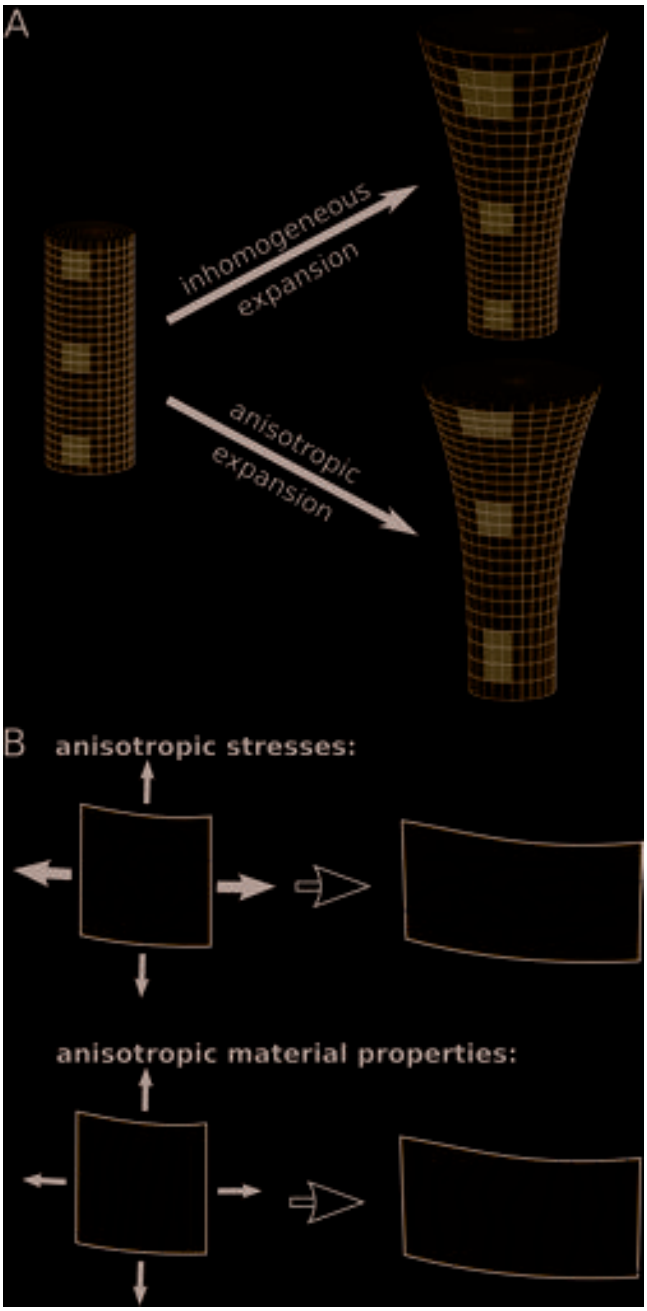

Fig. 1. Limits on the geometrical characterization of wall deformation. (A) Two contrasting ways to deform a cylindrical cell into a flaring trumpet (based on Green, 1969). Three wall patches illustrate the local pattern of surface deformation. For inhomogeneous expansion, shape change results from a gradient in the degree of area expansion. The three patches enlarge to varying degrees but remain approximately square. For anisotropic expansion, there is no gradient in area expansion (final wall patches have all the same area), but there is a gradient in the anisotropy or direction of expansion. (B) Two ways to deform a wall element anisotropically: using anisotropic stresses on an isotropic cell wall (top) or using isotropic stresses on an anisotropic cell wall (bottom). Macroscopically, the deformations are identical but at the microstructural level, the deformations proceed from distinct mechanisms.

The walled cell: a diagram of forces in equilibrium

D'Arcy W. Thompson (1942) famously said that organic form is a 'diagram of forces in equilibrium'. This description is

particularly accurate for the shape of walled cells. The cell wall evolved to bear the force of turgor pressure and is among the stiffest structures present within cells. Like any other material, the cell wall deforms only to the extent that forces are acting on it. The nature and extent of these forces play a major role in how the cell surface deforms and grows. However, as implied by Thompson's statement, the forces applied on the cell surface are balanced by counteracting forces in the wall, i.e. they are in equilibrium. In the simple case of a turgid and non-growing cell, turgor pressure is balanced by tensions in the polymeric network constituting the wall. For a given pressure, the cell can respond in many different ways depending on the constitution of its wall. The so-called constitutive properties of the wall material or the mechanism of wall deformation are the basis of the classification presented here. The idea of focusing on the constitutive response of the wall material is not new, as it is, implicitly or explicitly, the starting point of all mechanical analyses. However, in cell biology, this approach has not been used systematically to identify different modes of morphogenesis.

The modes of deformation considered here are those that emerge from different constitutive behaviours of the wall rather than their geometrical attributes (Fig. 2). The geometrical features that are sometimes used in defining a mode of deformation (e.g. inextensibility) are those that arise from a definite deformation mechanism and leave little doubt about the constitutive properties of the wall. Finally, the presentation sequence is meant to follow increasing degrees of freedom in deforming the cell wall (Fig. 2). Accordingly, I have adopted as a starting point (mode 0), a rigid wall that excludes any type of deformation.

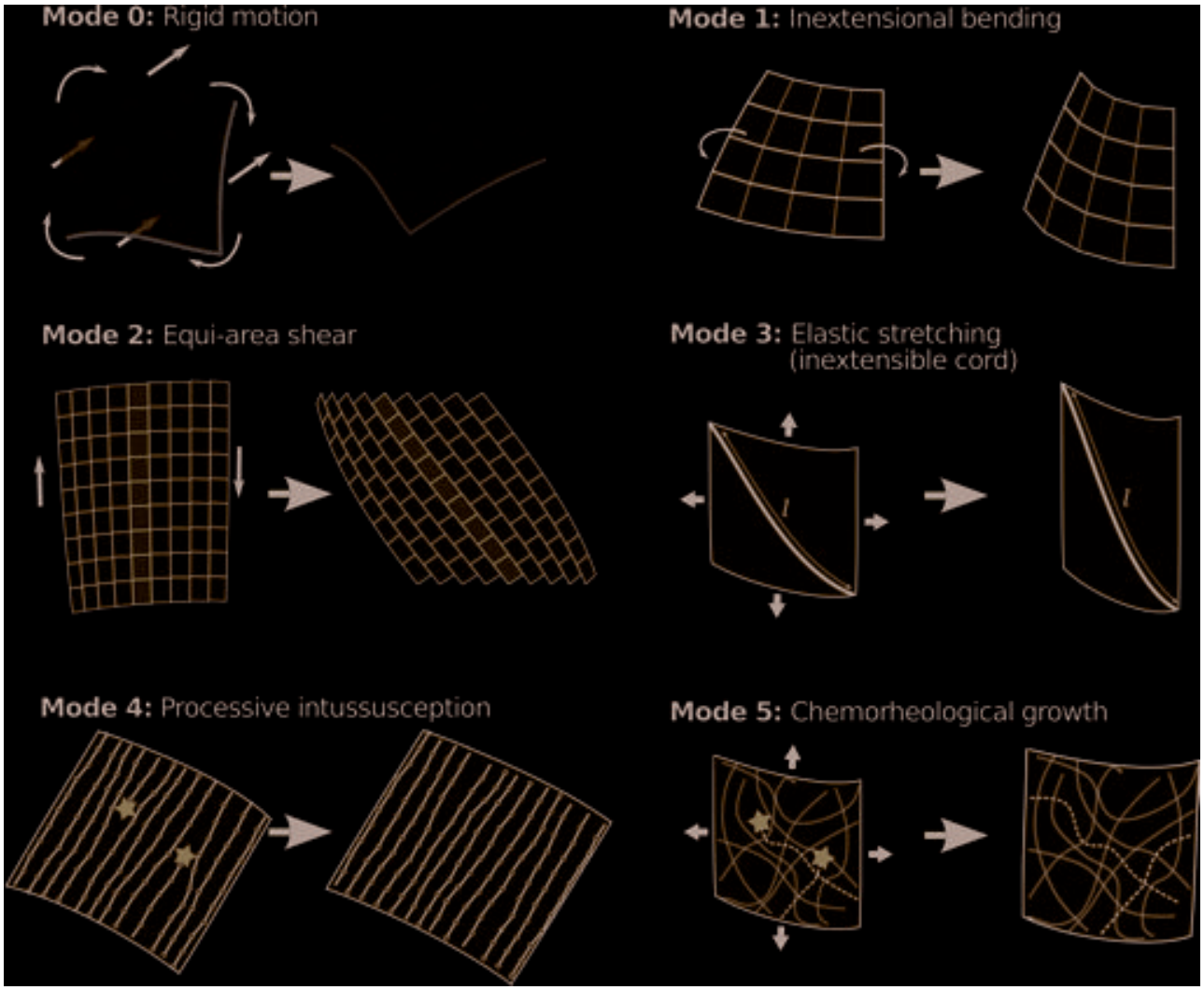

Fig. 2. Modes of deformation of cell walls. The modes are ordered roughly from the least to the most deformable wall. Mode 0 is a rigid wall element that will not undergo any deformation. All motions can be described as the sum of a solid body displacement and a rotation. Mode 1 is an inextensional bending that preserves all the length within the plane of the wall. Mode 2 is an equi-area shear. The length and width of the strips are conserved, but the strips are allowed to slide with respect to each other. Mode 3 is an elastic stretching, here illustrated in the special case where a family of inextensible cords is present (i.e. *l* is constant during the deformation). Mode 4 is a processive intussusception of new wall material by enzyme complexes (stars). Mode 5 is a chemorheological growth process where turgor stresses and the rate of wall deposition by secretion and wall synthesis (stars) contribute to the deformation.

Mode 0: rigid walls

Imagine a wall element that is not growing and cannot stretch or bend in any way. Such a wall element is undeformable and can solely undergo rigid body rotations and translations (Fig. 2, mode 0). A cell confined by a continuous layer of this rigid material would be prisoner of its own wall. This explains why most rigid walls are articulated in some way. They come either in the form of overlapping plates (e.g. the scales of coccolithophores) or of imbricating elements (e.g. the frustules of diatoms). Moreover, these rigid walls, unable to deform, must be 'assembled' using an organic template as a mould. In diatoms, assembly of the frustule is performed within the silica deposition vesicle where adjacent areolar vesicles help control the deposition of the silica to form the frustule (Pickett-Heaps *et al.*, 1990). For coccolithophore scales, a cellulosic base plate helps define the size and overall symmetry of the future calcium carbonate scale, while many of the finer details of the inorganic scale come from accretion at the surface of $CaCO_3$ crystals (Marsh, 2003; Henriksen *et al.*, 2004; Henriksen and Stipp 2009).

The inability of a cell to remodel its wall leads to unusual strategies to accommodate growth and mitosis. In the most extreme cases, the cell must escape the protection of its own wall in order to grow, as in foraminifers (Spero, 1988). In diatoms, the cell's inability to remodel its wall leads to a reduction in size at each cell division; these cells would vanish if it were not for periodic rounds of sexual reproduction that restore their original size (Pickett-Heaps *et al.*, 1990).

Mode 1: inextensional bending

I next consider a wall that cannot stretch. More specifically, I consider a thin wall whose mid-plane does not allow any length changes (Fig. 2, mode 1). If it is deformed, the deformation must be length preserving. For such a wall, the only possible deformation is bending, i.e. a change in the curvature of the mid-plane. A sheet of paper is a good analogue of an inextensible wall. Because it is thin, the sheet can bend or fold easily; however, most sheets of paper are sufficiently stiff to prevent any significant stretching. If we were to draw a series of lines on the sheet, no amount of folding and bending would alter the length of these lines.

Under what conditions would the constitutive behaviour of the wall approximate inextensibility? Certainly, a convex cell cannot increase its volume without at the same time stretching its wall. Inextensibility is not a mode of deformation that is compatible with cell expansion. In contrast, when a walled cell deforms because it loses volume, say, as a result of desiccation, its wall may comply with the decreasing volume by inextensional bending. Some examples of inextensional deformation with functional significance include the spores of some eusporangiate ferns (Hovenkamp *et al.*, 2009) and the annular cells of fern leptosporangia (Noblin *et al.*, 2012). However, the best illustration of this mode of deformation is the angiosperm pollen grain whose entire suite of structural adaptations seems to be tailored to favour large-scale inextensional bending of its wall (Halbritter and Hesse, 2004; Katifori *et al.*, 2010; Couturier *et al.*, 2013).

Pollen grains are live cells that must leave the protective environment of the anther during the pollination process. As with all living cells, their small size makes them vulnerable to rapid desiccation when exposed to air. The danger of dehydration remains until the pollen grain lands on the stigma where it can absorb water before germinating to complete fertilization. Without any protective mechanism against desiccation, most pollen grains arriving at the stigma would be dead or would be in a state of deep dormancy that would preclude quick germination and passing on their genes to the next generation.

The near-universal solution to the desiccation problem is harmomegathy (Vesque, 1883; Wodehouse, 1935; Bolick, 1981). Harmomegathy is the characteristic infolding of the pollen grain's apertures in response to a decreasing cellular volume (Fig. 3A–C). The apertures on the pollen surface provide the main routes for water exchange because, unlike the exine present elsewhere on the pollen surface, their cellulosic wall is not impregnated with sporopollenin and thus remains permeable to water (Heslop-Harrison, 1979*a*,*b*). The structure of the pollen wall is designed to allow the apertures to fold inwardly during harmomegathy, thus reducing the rate of water loss (Fig. 3C). Specifically, the apertures function as local soft spots that guide various pollen grains along specific folding pathways (Katifori *et al.*, 2010). For thin shells, bending modes of deformation (i.e. the modes that change the local curvatures of the surface) are known to be energetically less expensive than stretching modes (Box 1). Considering inextensional (bending-only) deformations of the wall, we can arrive at simple solutions for the folding of pollen grains. For a closed convex surface such as a sphere, at least two distinct types of inextensional deformation exist: a mirror reflection of a segment of the surface about a dissecting plane, and folding of the surface past a meridional slit (Fig. 3F). These two types of inextensional deformation provide a good approximation of the deformation observed in inaperturate and aperturate pollen grains, respectively (Fig. 3).

The requirement that the surface should not stretch has one important geometrical implication—the Gaussian curvature of the surface must be preserved during folding (Pogorelov, 1988). For an axisymmetric surface, the constant Gaussian curvature constraint leads to a simple relationship between the deformed and undeformed geometries (Katifori *et al.*, 2010):

$$r(s) = \alpha r_0(s) \tag{1}$$

where r and r_0 are the radial distances from the axis of rotation for the deformed and undeformed geometries and s is the meridional arc length (Fig. 4A). Here α is a parameter that sets the degree of closure.

This simple relationship can reproduce the folding of a pollen grain remarkably well (Fig. 4). For the lily pollen, gradually decreasing the parameter α from its initial value of 1 leads to the characteristic cigar shape observed during harmomegathy (Fig. 4A, B). For the triaperturate pollen of euphorbia,

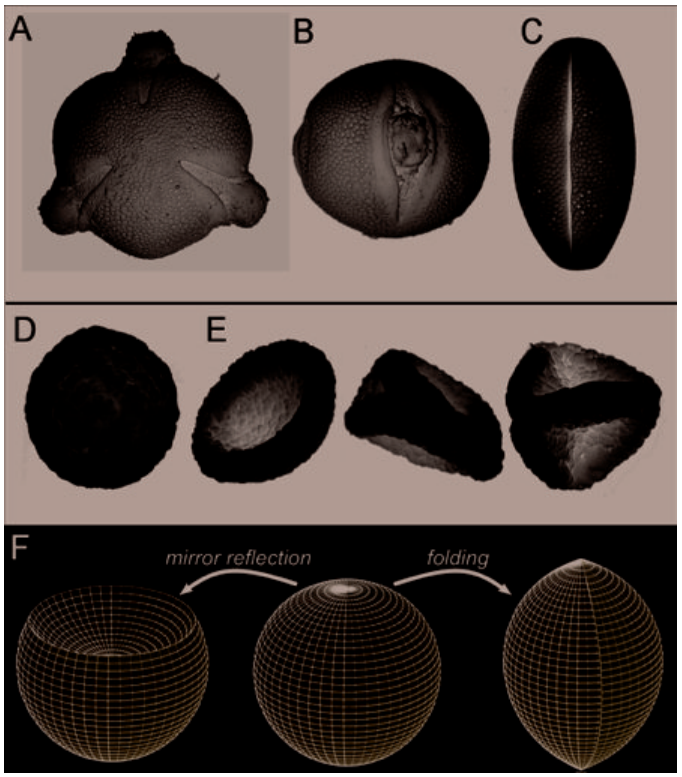

Fig. 3. Two examples of inextensional deformations in pollen grains. (A, B) Polar and equatorial view of the tri-aperturate pollen of *Euphobia milii* in its hydrated configuration (with the aperture exposed). (C) Equatorial view of the folded pollen with the aperture now retracted within the water-impermeable exine. (D) Inaperturate pollen of *Aristolochia gigantea* in its hydrated configuration. (E) Three examples of the inversion of the pollen surface in response to dehydration. (F) Two alternative inextensional deformations of the sphere. (A) and (B) were kindly provided by Dr Eleni Katifori.

Box 1. Thin shells favour bending over stretching

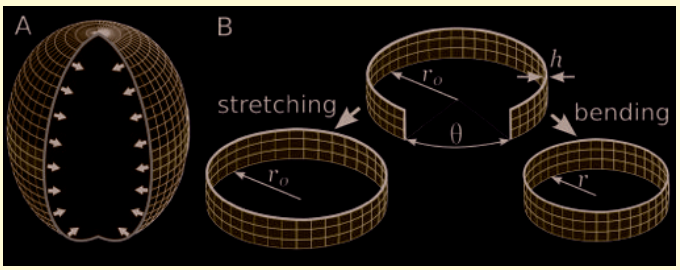

Surface elements within an elastic shell can respond to loads in two contrasting ways. They can stretch in the plane of the shell or they can bend (e.g. change their curvature). The question is, what is the best way to deform if the shell is thin, as most walled cells are. It is a well-known result that thin shells favour bending over stretching whenever the loading conditions allow it (Pogorelov, 1988). A simple calculation of the bending and stretching strains illustrates why it is so. Imagine a pollen grain where the edges of the aperture are being pulled toward each other (A) and consider how a narrow equatorial strip ought to deform. The strip can respond to this load by: (i) stretching over the aperture while keeping its radius constant, or (ii) bending into a tighter roll to close the gap (B). We can easily compute the strains associated with these two alternatives. The stretching strains are $\epsilon_s = \frac{\Delta l}{l} = \frac{\theta}{2\pi - \theta}$ and the bending strains are $\epsilon_b = h\Delta\kappa = \frac{h}{r_0}\frac{\theta}{2\pi - \theta}$, where $\Delta\kappa = \frac{1}{r_0} - \frac{1}{r}$ is the change in curvature and all other variables are illustrated in the figure. The ratio of bending to stretching strains is simply $\frac{\epsilon_b}{\epsilon_s} = \frac{h}{r_0}$. It is clear from this relation that, for a thin shell (i.e. $h << r_0$), the strains produced by bending are much smaller than those produced by stretching. What is true for this specific case is also true more generally—wall elements in a thin shell would rather bend than stretch whenever the loading conditions allow it.

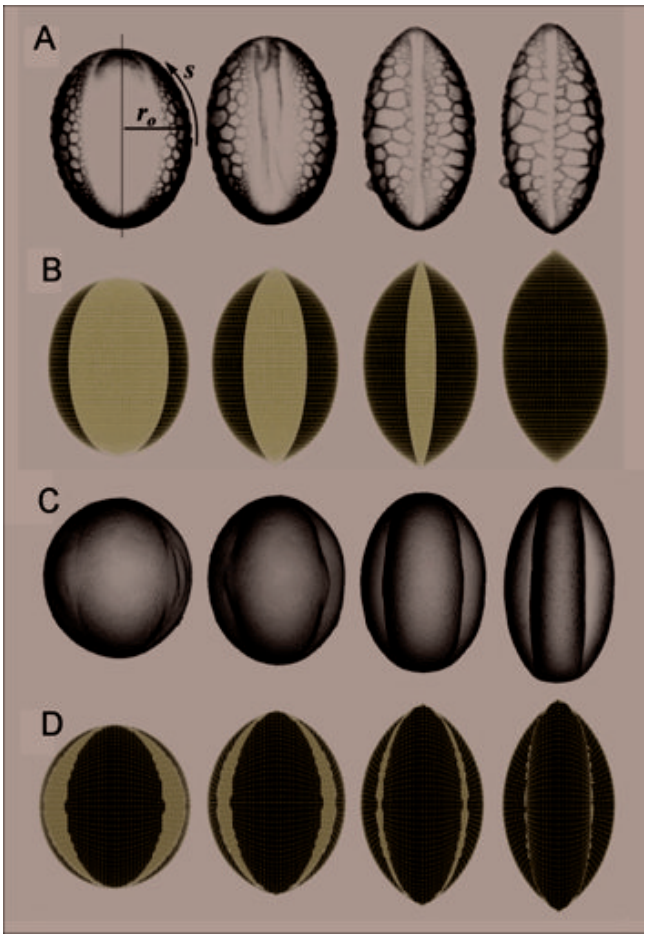

Fig. 4. Inextensional folding of pollen grains. (A) Folding of the monoaperturate pollen of lily. (B) Predicted inextensional folding for a surface with the same initial geometry and aperture opening as in (A). (C) Folding of the triaperturate pollen of euphorbia. (D) Predicted inextensional folding for a surface with the same initial geometry and aperture opening as in (C). From Katifori *et al.* (2010).

the surface is subdivided into three identical interapertural elements (Fig. 4D). Now increasing the parameter α above 1 leads to folding of these elements and closure of the pollen grain. The precise match between the closed-form solutions and the observed folding indicates that the dominant mode of deformation is consistent with an inextensional bending of the pollen wall.

The most striking conclusion of this analysis is that harmomegathy in pollen grains is governed entirely by the shape of the interapertural regions where the sporopollenin-impregnated wall is unable to stretch. Its inextensional deformation dictates how the hydrated shape is transformed into a folded—and sealed—shape.

Mode 2: equi-area shear

I next consider a mode of area-preserving deformation unique to euglenoid algae. Members of the genus *Euglena* and related algae are well known to undergo large body deformations when swimming in cluttered environments. The characteristic shape changes have been termed euglenoid movement or metaboly (Leedale *et al.*, 1965). Careful work by Suzaki and Williamson (1985, 1986) has highlighted the role of the pellicle in controlling euglenoid movement. The pellicle of euglenoids occupies the cortex of the cell and is comprised of long proteinaceous strips that are tightly imbricated and lined with microtubules at their point of juncture (Fig. 5A, B) (Leedale, 1964; Suzaki and Williamson, 1985). In *Euglena fusca*, these strips are approximately 100 μm long, 2 μm wide, and 0.3 μm thick. Although the pellicle is not a cell wall, its position in the cortex of the cell and its slenderness endow it with wall-like properties.

At first sight, the changes in cell shape are of such amplitude that one may wrongly conclude that the cortical pellicle exerts little influence on the deformation of the cell. Indeed, descriptions of euglenoid movement as 'a sort of amoeboid movement within the confines of an elastic pellicle of definite shape' (Leedale *et al.*, 1965) would suggest extensive freedom to change morphology. During the rhythmic contractions associated with euglenoid movement, the strips are observed to slide pass each other to and fro in a regular sinusoidal fashion with the same period as the movement itself (Suzaki and Williamson, 1985). At maximum cell rounding, the pellicular strips can be shifted by as much as 4 μm when compared with their relative alignment in an elongated cell. The lateral displacement of the strips

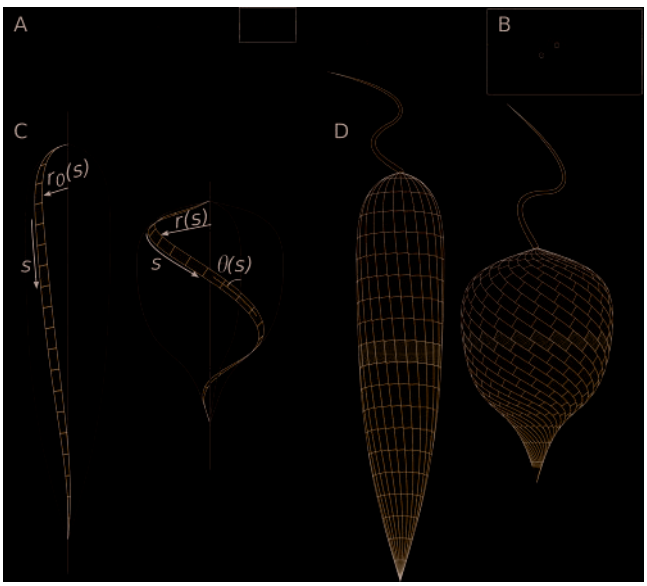

Fig. 5. Equi-area shear in *Euglena*. (A) Schematic cross-section of the pellicle of *Euglena fusca* showing four imbricated pellicular strips (based on Suzaki and Williamson, 1986). (B) Close-up of the articulation showing the plasma membrane (blue) and two strip-associated microtubules that are presumably responsible for the sliding of the strips. (C) Geometry of one pellicular strip in an elongated cell (left) and a rounded cell (right). (D) Overall geometry of an elongated cell and a rounded cell. For clarity, only 20 of the 40 or so strips are shown. The strips are shaded at one level to show the large shear that takes place between them during euglenoid movement.

with respect to their neighbours reaches a maximum in the middle of the cell and is absent at the anterior and posterior ends. In other words, the strips appear to be anchored at their extremities but able to slide passed each other elsewhere (Fig. 2, mode 2).

The relative sliding of the strips is to be contrasted with the complete absence of stretching within the strip themselves. A detailed analysis by Suzaki and Williamson (1985) showed that the distance between landmarks within a strip as well as the strip width are constant within experimental error. Therefore, the elements of the pellicle are not 'elastic' as claimed by some investigators but virtually inextensible under normal conditions. If the tightly imbricated strips do not change in number, length, or width during euglenoid movement, we must conclude that the surface area of the cell is constant.

In considering the range of deformation possible given the equi-area deformation mechanism of *Euglena*, I will focus only on axisymmetric shapes, but the reader can consult Suzaki and Williamson (1986) for a qualitative account of euglenoid movement involving periodic bending of the cell. As the pellicle strips do not change length during deformation, it is convenient to use the arc length along the strip, s, as an independent variable. In the elongated conformation, the strips very nearly line up with the meridians of the cell. The shape is thus fully determined by specifying the radial distance of the strips $r_0(s)$ (Fig. 5C, D). Sliding between two adjacent strips forces them to take a more oblique position with respect to the cell's meridians (Fig. 5C, D). If the width of the strips varies slowly over the length of the cell, a simple calculation shows that the radius of a deformed cell is:

$$r(s) = \frac{r_0(s)}{\cos\theta(s)} \qquad (2)$$

where $\theta(s)$ is the local angle between the strip and the cell's meridian. This relationship encapsulates the essence of equi-area deformation. The widening of the cell (i.e. greater r values) is contingent on the strips being more oblique to the cell's axis (greater angle θ), which in turn means the cell's axis is shorter, as the strips take a more tortuous path to join the anterior and posterior ends of the cell. Comparing this equation with Equation (1), we see that *Euglena* possesses additional degrees of freedom to control its shape, having just replaced the constant α of Equation (1) by the function $\cos\theta(s)$. However, not all functions $\theta(s)$ are appropriate. As shape changes occur rapidly, it is likely that the deformation occurs at nearly constant cytoplasmic volume. This constraint limits the range of possible functions $\theta(s)$.

One critical question remains: is sliding a passive response of the pellicle to forces generated within the cell or does sliding itself drive cell motility? The latter appears to be the case. Suzaki and Williamson (1985) proposed a deformation mechanism for *Euglena* that is very much like the beating of flagella, where shear between the nine outer microtubule doublets drives the bending of the axoneme (Bray, 2000). We thus conclude that euglenoid movement, far from being 'a sort of amoeboid movement within the confines of an elastic pellicle of definite shape', results from the active sliding of inextensible helical strips within the cell cortex.

Mode 3: elastic stretching

Any cell endowed with turgor pressure must have its wall distended elastically. Therefore, elastic deformation is the most ubiquitous mode of deformation found in walled cells (Fig. 2, mode 3). Although few cells can undergo large elastic deformations, wall elasticity appears to be involved in the morphogenesis, movement, and function of many cells. One well-studied example is the elastic deformation of guard cells within the stomatal complexes of plants (Franks *et al.* 1998), while many other examples are encountered in prokaryotes (Trachtenberg *et al.*, 2003; Wolgemuth *et al.*, 2005; Cabeen *et al.*, 2009; Dombrowski *et al.*, 2009).

The possible range of elastic deformation in a cell is very broad and cannot be encapsulated in a simple formula like the two modes of deformation discussed above. The unifying principle for all elastic deformations is the minimization of elastic energy (Landau and Lifshitz, 1986). For a given load and set of material properties, a wall element will take the geometry that minimizes its elastic energy. The minimization of the elastic energy of the cell is the other face of the force equilibrium advocated by D'Arcy Thompson. The minimal energy requirement imposes a particular morphogenetic challenge for cells that are loaded by internal turgor pressure. If the wall surrounding the cell is both isotropic and homogeneous, pressure loading leads invariably to a deformed cell that is closer to being spherical than the initial cell geometry (Box 2). In the many instances where cellular function depends on attaining a non-spherical geometry, the cell must modulate the properties of its wall either in terms of structural anisotropy or in terms of spatial inhomogeneities to depart from the spherical shape. In fact, most of the structural features observed in the wall of turgid cells, such as reinforcement by fibres, are directly or indirectly related to the need to counter the spherical tendency imparted by turgor loading.

Fibre-reinforced cylindrical hydrostats

To highlight the role of wall structure in guiding surface deformation and cell geometry, I consider a limiting case where some fibres within the wall are of such stiffness that even a small strain within these fibres would cause the elastic energy to grow rapidly. In such a wall, we can expect deformations that leave the fibre length constant. One particularly rich case is a cylindrical cell reinforced by a family of helical fibres (Fig. 6). A cell reinforced in this way has a limited range of shapes it can take when loaded by internal pressure. The typical response is one of axial twisting and stretching in the transverse direction (Fig. 6A). This response is reminiscent of the so-called helical growth of *Nitella* (Green, 1954),

Box 2. Pressure loading favours spheres

The tendency of pressure-driven deformations to make shells more spherical ought to seem familiar to anyone who has ever inflated a rubber balloon. One way to understand this response is through the well-known fact that a sphere maximizes the volume for a given surface area. If a cell of any shape is subjected to an increase in volume, it can minimize the amount of added strains to its wall, and therefore the total elastic energy, by accommodating this new volume in a mode of deformation that brings its shape closer to the sphere. In other words, pressurized shells do not accommodate added volume by sprouting narrow extensions but by rounding up as much as possible, at least as long as their material properties remain isotropic and homogeneous.

An alternative way to explain the spherical tendency is through Laplace's Law, which describes the balance of forces between pressure (P) and wall tensions (T_1) in a doubly curved shell:

$$P = T_1\kappa_1 + T_2\kappa_2 \quad (3)$$

where κ_1 and κ_2 are the local curvatures. According to Laplace's Law, the wall tensions are, on average, highest where the curvatures are lowest, as pressure itself is constant everywhere. The local high tensions force the shell to bulge out or curve more, thus bringing the lowest curvature closer to the average curvature of the shell. This 'equilibration' process stops when the curvature is equal over the entire shell surface, i.e. when the shell is spherical. To achieve shapes that are non-spherical, elastic shells and walled cells must use material anisotropy and inhomogeneity in their wall.

Phycomyces (Castle, 1942; Wold and Gamow, 1992), and some bacterial cells such as *Escherichia coli* (Wang *et al.*, 2012).

Now assume that only one fibre is inextensible. This arrangement breaks the symmetry of the system and therefore forces the cylinder to take on a more complex shape to accommodate any increase in volume (Fig. 6B, C). If the fibre angle is zero, the cylinder may deform into a planar arc (Fig. 6B). On the other hand, if the unique fibre forms a helix around the cylindrical cell, an increase in volume can be accommodated by straightening (without stretching) the fibre and winding the cell cylinder around it (Fig. 6C). Variations upon this theme have been used to explain the morphology and locomotion of many prokaryotes (Trachtenberg *et al.*, 2003; Wolgemuth *et al.*, 2005; Cabeen *et al.*, 2009; Dombrowski *et al.*, 2009).

Mode 4: processive intussusception

I consider now the important case of growth deformations and, in particular, a mode of growth where the cell maintains direct molecular control over the expansion of its surface, i.e. the increase in wall area is achieved by inserting new molecular units within a regularly arranged wall monolayer (Fig. 2, mode 4). This mode of growth is the purest form of *intussusception*, a term coined by Karl Nägeli to describe a process of wall expansion whereby new wall material gets inserted within the pre-existing wall fabric, thus expanding its surface area. I will call this mode of wall deformation processive intussusception. Two examples to be considered are the highly regular surface layers (S-layers) and peptidoglycan walls of many prokaryotes (Fig. 7). A processive intussusception mechanism is analogous to DNA replication where 'processivity' refers to the number of nucleotides that are copied within one run of the enzyme DNA polymerase. During replication, the molecular machinery walks along doubled-stranded DNA, separating and duplicating the two strands, thus yielding double the amount of DNA. Similarly, the wall assembly machinery of a processive growth mechanism has to track a specific wall element while cutting load-bearing bonds and inserting new material to bridge the gap created. Processivity comes into play because of the need to maintain the structural anisotropy present in the wall (Wang *et al.*, 2012). A more distributive mode of insertion would ultimately destroy the structural anisotropy of the wall and impair the ability of the cell to control the direction of wall insertion and the overall growth pattern.

S-layers

The term 'surface layer' or 'S-layer' refers to a specific wall layer encountered in many prokaryotes that is composed of proteins arranged into a closed two-dimensional lattice of near-crystalline regularity (Fig. 7A, B). Interestingly, similar crystalline layers are also seen in *Chlamydomonas* and other volvocine algae (Roberts *et al.*, 1985; Woessner and Goodenough, 1994). Soon after S-layers were discovered, the problem of their growth was considered (Houwink, 1956). As most crystals grow by accretion of new molecular units at their free faces, one may ask how a nearly crystalline wall would grow. After all, a closed two-dimensional crystal has no free edge where new particles could be aggregated to increase surface area. Houwink (1956) proposed that points of dislocation and disclination within the lattice could act as growth foci. This idea was later developed by Harris and Scriven (Harris, 1970; Harris and Scriven, 1970, 1971) and Pum *et al.* (1991).

One possible mechanism of intussusception would be through the movement of a complementary pair of disclinations—a fivefold vertex and a sevenfold vertex within the regular hexagonal lattice observed in many S-layers (Fig. 8A–D) (Pum *et al.*, 1991). The protein components in the neighbourhood of the disclination find themselves in a state of quasi-equivalence (Caspar and Klug, 1962), i.e. their bonding interactions, although not exactly equivalent to those of a regular hexagonal lattice, remain close to the presumably optimal sixfold symmetry. The slight variations in the local

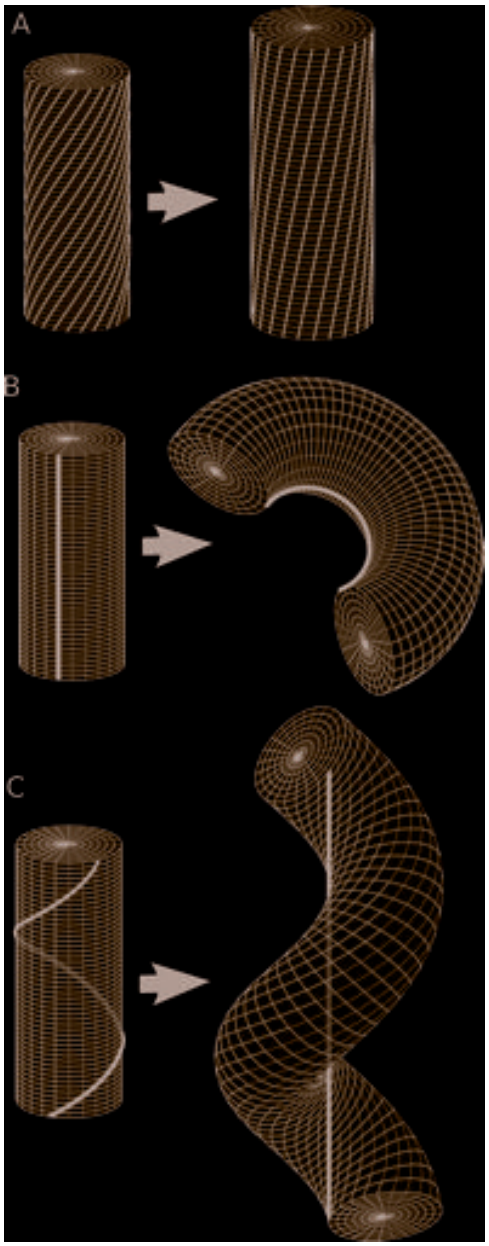

Fig. 6. Deformation of cylindrical cells reinforced by inextensible fibres. (A) A family of inextensible fibres (shown in bold) wrapped helically around a cylindrical cell. When loaded by turgor pressure, such cells expand by untwisting of the fibres while remaining cylindrical. (B) Bending of a cylindrical cell reinforced by one fibre aligned with the cell generators. (C) Twisting and bending of a cell reinforced by one fibre wound helically around the cell.

bond lengths associated with the points of fivefold and sevenfold symmetry lead to a locally elevated strain energy, which may help promote the insertion of new units at this location. The intussusception of new protein units would follow a well-defined path, pushing the complementary pair along one of the lattice axes (Fig. 8A–D). This processive insertion of new units offers an elegant explanation for the long-range regularity of S-layers. A more stochastic or distributive mode of assembly would lead to the polycrystal structure observed *in vitro* but not seen in living cells (Chung *et al.*, 2010).

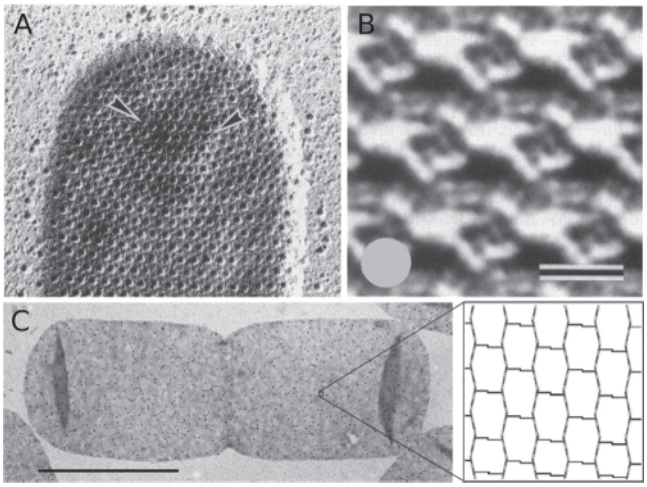

Fig. 7. Ordered wall layers in prokaryotes. (A, B) The S-layer of *Thermoproteus tenax* (from Messner *et al.*, 1986. Copyright © American Society for Microbiology, *Journal of Bacteriology* **166** number, 1986, 1046–1054). The two arrowheads in (A) indicate disclinations. In (B), a higher magnification of the S-layer is shown. Copyright © American Society for Microbiology, *Journal of Bacteriology* **166** number, 1986, 1046–1054. (C) Sacculus of an *E. coli* cell in the process of division (from Vollmer and Bertche, 2008). The insert shows the typical wall structure with the glycan strands running vertical and the peptide cross-links running horizontal. Bars, 25 nm (B); 1 μm (C). Reprinted from *Biochimica et Biophysica Acta* 1778, Vollmer W, Bertsche U. Murein (peptidoglycan) structure, architecture and biosynthesis in *Escherichia coli*, 1714–1734. Copyright with permission from Elsevier.

One consequence of this mode of wall growth is that large segments of the S-layer must be inherited from generation to generation. Several papers have indeed confirmed that the proteins in the S-layers do not turn over (Howard *et al.*, 1982). The stability of the S-layer once assembled is most clearly seen at the cell ends, which are inherited, apparently intact, for multiple generations (Acosta *et al.*, 2012). Finally, although S-layers can self-assemble *in vitro* to form regular lattices, the overall shape of a cell covered with an S-layer does not reflect the crystal symmetries present within the layer itself. Thus, the shape of even the smallest eubacteria or archaea is not self-assembled in the same way that a virus capsid is (Crick and Watson, 1956; Caspar and Klug, 1962).

Peptidoglycan walls

The sacculus of Gram-negative bacteria such as *E. coli* is thought to represent a monolayer of circumferentially aligned glycan strands cross-linked by short peptide chains (Fig. 7C) (Vollmer and Bertsche, 2008). Although not a crystalline lattice like the S-layers discussed above, the microstructural regularity of the sacculus goes far beyond that of other cell walls. As a result of this regular wall structure, the principal stress components can be supported by specific intermolecular bonds, i.e. the axial stress is supported primarily by the peptide chains and the circumferential stress is supported by the glycan strands. It is therefore possible to control growth anisotropy at the molecular

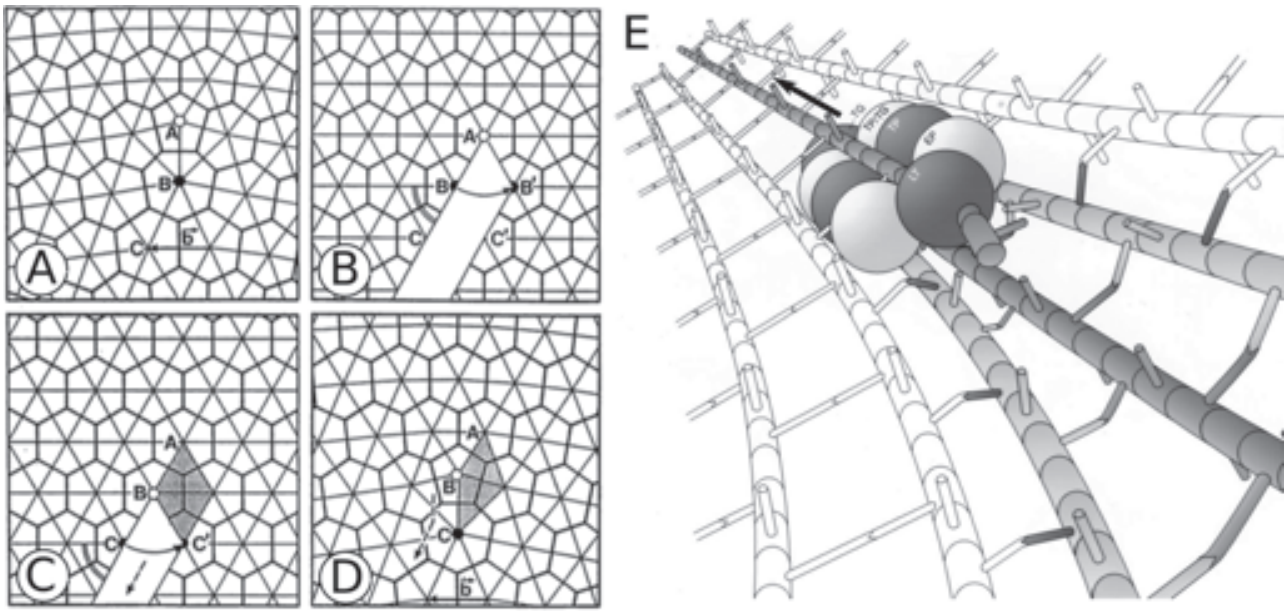

Fig. 8. Processive intussusception in prokaryote cell walls. (A–D) Intussusception through the processive movement of a disclination pair (from Pum *et al.*, 1991). Copyright © American Society for Microbiology, *Journal of Bacteriology* **173**, 1991, 6865–6873. (A) A complementary pair of disclinations (fivefold and sevenfold vertices) within a regular hexagonal lattice. (B, C) Schematic showing how opening of the lattice along the axis joining the disclination pairs can make room for a new wall element (shown here, hypothetically, as a diamond shaped element). (D) Closing of the lattice with this new element in place leads to the same complementary pair but now advanced one step forward. (E) The three-for-one model of peptidoglycan wall assembly (from Höltje, 1998). Following this model, the wall assembly machinery travels along one docking glycan strand, depolymerizing the docking strand as it progresses forward and synthesizing three new strands to replace it. A net growth of two glycan chains is thus achieved. Copyright © American Society for Microbiology, *Microbiology and Molecular Biology Reviews* **62**, 1998, 181–203.

level by selectively breaking the peptide bonds and inserting new glycan strands (Fig. 8E) (Höltje, 1998). Although the details of the wall assembly process remain unclear, the processive nature of the sacculus growth has been elegantly demonstrated by *in vivo* labelling of the MreB cytoskeletal proteins and of the wall assembly machinery in *Bacillus subtilis* (Sliusarenko *et al.* 2010; Domínguez-Escobar *et al.*, 2011; Garner *et al.*, 2011).

As shown by Amir and Nelson (2012), processive intussusception leads to a simple equation for how the rate of cell elongation is controlled by wall assembly. Focusing on the change in length (l) of a cylindrical cell such as *E. coli*, the relative rate of elongation or strain rate ($\dot{\varepsilon}$) is given by the equation:

$$\dot{\varepsilon} = \frac{1}{l}\frac{dl}{dt} = nvd \qquad (4)$$

where n is the area density of sites of active wall insertion, v is the velocity of those sites, and d is the amount of axial length that is added at each insertion site. For example, the three-for-one model illustrated in Fig. 8E would add a net axial length equivalent to twice the typical axial spacing between glycan chains (i.e. one strand is removed while three are added). Under favourable growth conditions, it is assumed that the parameters of Equation (4) are constant and therefore the length of the cell should increase exponentially in time, which is confirmed by observations (Wang *et al.*, 2010). Equation 4 highlights two interesting and rather unique features of intussusceptive growth (Harris, 1970): (i) growth occurs at well-defined and persistent foci on the cell surface, and (ii) the addition of material follows a specific direction, which ultimately controls the direction of cell-surface expansion. These features are made possible by the uniquely regular organization of some bacterial walls. As we shall see in the next section, the more complex wall organization of other cell types precludes such direct control over wall assembly and wall expansion, although wall assembly in those cells may still share some fundamental similarities with processive intussusception.

Mode 5: chemorheological growth

Under this heading, I include the growth of a broad class of walled cells, including the two classic cases of tip growth and diffuse growth. The control of cell enlargement in plants has been reviewed on many occasions (Ray, 1987, 1992; Cosgrove, 1997, 2005; Baskin, 2005; Geitmann and Ortega, 2009) so it is not my intention to provide an in-depth treatment of this topic. Instead, I want to concentrate on the possible role of chemorheology in the growth of plant cell walls and draw a parallel with the mode of expansion observed in some prokaryotes.

Chemorheology is the chemically mediated flow of a polymeric materials. The formalism of chemorheology is well adapted to a material whose rate of flow is dependent on the

rate of chemical reaction within it, as would be the case if bonds need to be severed to allow a cross-linked polymeric material to flow in response to the stress applied to it (Ray, 1992). For plant cells, two polymer networks may contribute to chemorheology. In the Ca^{2+}–pectate network, two de-esterified residues of polygalacturonan can form a cross-link by binding a single Ca^{2+} ion (Schols and Voragen, 2002). As suggested by the work of Boyer and co-workers in the large *Chara* internodal cell, free binding sites on newly de-esterified pectins may be able to compete for Ca^{2+} ions with load-bearing Ca^{2+}–pectate cross-links, thereby relaxing the stress present in those bonds and allowing the wall to deform (Proseus and Boyer, 2006; Boyer 2009). If such competition is the dominant mode of stress relaxation in the wall, the rate of deformation of the pectin matrix must reflect the rate at which load-bearing cross-links are severed by de-esterified but as yet uncrosslinked pectins, i.e. relaxation is chemorheologically controlled. Interestingly, experiments performed over 50 years ago led Cormack (1949, 1954) to put forward a similar proposal for root hairs. More recent work on the shoot apical meristem also supports a role for the Ca^{2+}–pectate network in controlling wall expansion (Peaucelle *et al.*, 2012; Braybrook and Peaucelle, 2013). Pectins may therefore play a role in wall expansion beyond the charophytes.

The parallel network of cellulose and hemicelluloses may also behave as a chemorheological material. It is believe that xyloglucan chains in the wall serve to tether cellulose microfibrils and thus provide a coherent network to support the internal turgor pressure of the cell. In view of the important mechanical role of xyloglucans, the ability of endotransglucosylase/hydrolase enzymes to cut and rejoin xyloglucan chains suggests that plant cells can control directly the loosening of their walls (Fry, 2004). Given that the transglucosylase activity is often correlated with the growth rate of plant structures (Fry *et al.*, 1992), we have here all the conditions necessary for chemorheological control of wall growth. Other wall proteins such as expansins may also contribute to wall relaxation (Cosgrove, 2000).

Mechanistically, chemorheology is to be contrasted with, on the one hand the processive intussusception described above, and on the other hand the flow of a viscous material. In processive intussusception, the regularity of the wall matrix is such that insertion of wall material in and of itself determines the deformation (Fig. 8). The strict intussusceptive control of wall deformation is most clearly seen for the S-layer, as every protein unit inserted in the wall contributes a well-defined area of cell surface (Fig. 8A–D). In contrast, although chemorheology can also lead to intussusception of new wall material, the inserted material is presumed to be amorphous or sufficiently flexible to fill the voids opened by the breaking of load-bearing bonds. Thus, wall deformation is dictated by the local elastic relaxation that follows the breaking of bonds rather than by the 'shape' of the material deposited.

Chemorheology should not be equated with viscous flow either. In a viscous material, deformation relies on the relative displacement of weakly interacting molecules, not on the rate of chemical reactions within the load-bearing network. This distinction is highlighted by the strong temperature dependence of wall growth, which is indicative of underlying chemical reactions (Ray and Ruesink, 1962; Proseus *et al.*, 2000). For example, Ray and Ruesink (1962) observed a threefold change in elongation rate for a 10 °C change in temperature. For comparison, the temperature dependence of the creep rate in boiled oat coleoptiles (Cleland, 1971) and isolated *Chara* cell walls (Haughton and Sellen, 1969) is minimal, as is the temperature dependence of most viscous materials far from their glass transition. Although cell walls do have a true viscosity over short time scales, the chemorheological growth of the cell wall over a long time scale has only the appearance of a viscosity (Dumais *et al.*, 2006; Rojas *et al.*, 2011), and the cell's ability to expand would be lost rapidly if the chemical reactions supporting the remodelling of the wall were stopped.

In the context of the pectic wall of pollen tubes, Rojas *et al.* (2011) have proposed a simple relation for the chemorheological strain rate ($\dot{\varepsilon}_i$) of the wall:

$$\dot{\varepsilon}_i = \tau \varepsilon_i \tag{5}$$

where ε_i is the elastic strain of the load-bearing polymers and τ is the rate at which bonds are exchanged between the load-bearing wall network and newly deposited, and therefore relaxed, polymer chains. Equation (5) has several implications, one of which is that the ratio of strain rates between orthogonal directions on the cell surface must be equal to the ratio of elastic strains. This prediction was tested and shown to be accurate (Fig. 9) (Rojas *et al.*, 2011). Moreover, the strain profile observed in pollen tubes (Fig. 9B) is similar to those reported for other tip-growing cells including root hairs (Shaw *et al.*, 2000; Dumais *et al.*, 2004; Bernal *et al.*, 2007), the *Chara* and *Nitella* rhizoid (Hejnowicz *et al.*, 1977), and the sporangiophore of *Phycomyces* (Castle, 1958). It is therefore possible that the chemorheological model developed for the pectin wall of pollen tubes can in fact be applied over a broader range of organisms and wall microstructures.

Finally, an interesting aspect of chemorheology is that deposition of new wall material could, by itself, be sufficient to promote wall expansion (Ray, 1992). Wall polymers such as pectins and cellulose microfibrils are added to the wall without any prior cross-links. They therefore present, or will present after de-methylation in the case of pectins, free binding sites that are ready to be cross-linked. When juxtaposed with the pre-existing polymer chains, the new wall components could plausibly become cross-linked by exchanging their bonding capabilities for those of previously deposited polymers. As the cross-links already present in the wall are likely to be under tension, and the substitution with a new wall element would relax this tension, one may expect the exchange to be favoured thermodynamically.

This particular version of chemorheology closely follows the processive intussusception mechanism described above but for one notable difference: the new wall material is deposited in an amorphous state rather than neatly inserted along a specific wall direction. This amorphous material takes form only through the relaxation of the local elastic

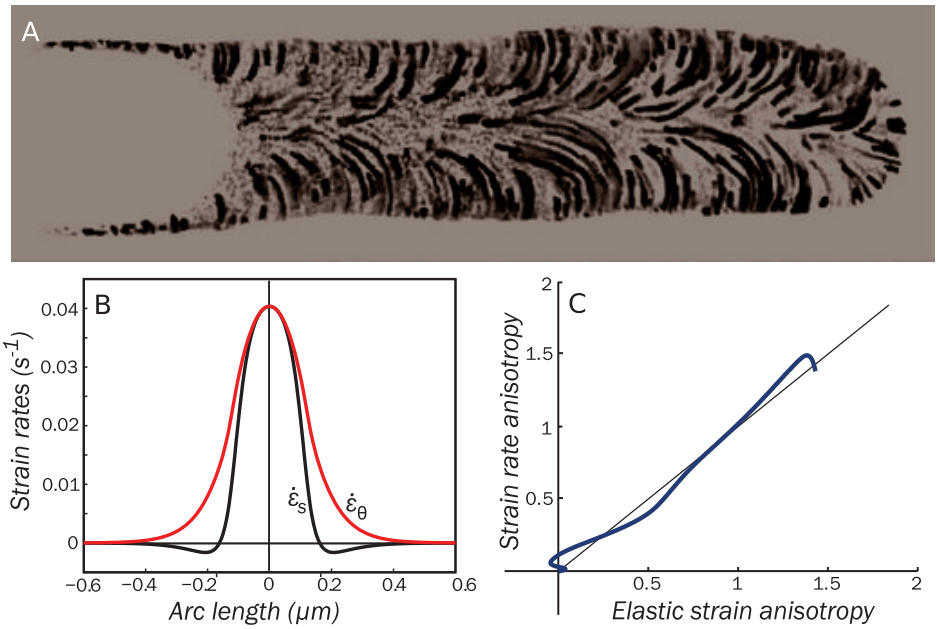

Fig. 9. Relationship between wall strain rates and elastic strains in the pectic wall of lily pollen tubes. (A) A fluorescently labelled pollen tube showing the displacement of a material point on the cell surface during the growth process. (B) Strain rates extracted from the fluorescent markers in (A). (C) Comparison between the measured strain rate anisotropy and the predicted elastic strain anisotropy based on the wall stresses. The two variables follow each other very closely (Reprinted from Biophysical Journal 101, Rojas ER, Hotton S, Dumais J. 2011. 1844–1853. Chemically-mediated mechanical expansion of the pollen tube cell wall). Copyright with permission from Elsevier.

strains. Although a mechanism of this type is unlikely to be the sole contributor to wall growth, it has the added benefit, just as with processive intussusception, that wall expansion is in direct proportion to the amount of new wall material added to it. Thus, the mechanical integrity of the wall is never endangered, as it would be if the breaking of cross-links was out of pace with the addition of new wall material and the formation of new cross-links.

Conclusions

This survey illustrates the great diversity of wall-deformation mechanisms present in walled cells. At one end of the spectrum lie the inextensional bending of pollen grains and the equi-area shear of euglenoids. For these two modes of deformation, the constraints are so severe that the realizable shapes can be expressed explicitly in terms of the resting geometry of the cell and other geometrical parameters. None the less, the range of shapes achieved by these cells is vast and appears particularly well suited for their functions in protecting the cell from desiccation in the case of pollen grains (Katifori *et al.*, 2010; Couturier *et al.*, 2013) and in effecting locomotion in the case of euglenoids (Arroyo *et al.*, 2012).

The wall growth mechanisms lie at the other end of the spectrum. These allow much greater flexibility in deforming the cell surface and are also more challenging to formalize mathematically. The processive intussusception found in prokaryotes, because of its inherent regularity, is the most tractable growth process and may serve as a model for the chemorheological growth of more complex cell walls. In both cases, one could argue that an increase in wall area is proportional to the mass or amount of material inserted in the wall. Yet one fundamental distinction exists in how growth anisotropy is produced. In the case of processive growth, the strain rate anisotropy is strictly defined by the mode of insertion of new wall material, i.e. the intrinsic structural anisotropy of the wall also specifies the deformation anisotropy. In contrast, the strain rate anisotropy observed in chemorheological growth does not emerge from the mode of insertion of new wall material; rather, it reflects the anisotropy of the elastic strains present in the wall. These two contrasting strategies to control the direction of growth emphasize the importance of looking beyond kinematics when analysing the modes of deformation of walled cells.

Acknowledgements

Some of these ideas were developed as part of a grant from the Human Frontiers Science Program.

References

Acosta F, Alvarez L, Angel de Pedro M, Berenguer J. 2012. Localized synthesis of the outer envelope from *Thermus thermophilus*. *Extremophiles* **16,** 267–275.

Amir A, Nelson DR. 2012. Dislocation-mediated growth of bacterial cell walls. *Proceedings of the National Academy of Sciences, USA* **109,** 9833–9838.

Arroyo M, Heltai L, Millán D, DeSimone A. 2012. Reverse engineering the euglenoid movement. *Proceedings of the National Academy of Sciences, USA* **109,** 17874–17879.

Baskin TI. 2005. Anisotropic expansion of the plant cell wall. *Annual Reviews of Cell and Developmental Biology* **21,** 203–222.

Bernal RV, Rojas ER, Dumais J. 2007. The mechanics of tip growth morphogenesis: what we have learned from rubber balloons. *Journal of Mechanics of Materials and Structures* **2,** 1157–1168.

Bolick MR. 1981. Mechanics as an aid to interpreting pollen structure and function. *Review of Palaeobotany and Palynology* **35,** 61–79.

Boyer JS. 2009. Cell wall biosynthesis and the molecular mechanism of plant enlargement. *Functional Plant Biology* **36,** 383–394.

Bray D. 2000. *Cell movements: from molecules to motility* . New York: Garland Press.

Braybrook SA, Peaucelle A. 2013. Mechano-chemical aspects of organ formation in *Arabidopsis thaliana:* the relationship between auxin and pectin. *PLoS ONE* **8,** e57813.

Cabeen MT, Charbon G, Vollmer W, Born P, Ausmees N, Weibel DB, Jacobs-Wagner C. 2009. Bacterial cell curvature through mechanical control of cell growth. *EMBO Journal* **28,** 1208–1219.

Caspar DLD, Klug A. 1962. Physical principles in the construction of regular viruses. *Cold Spring Harbor Symposia on Quantitative Biology* **27,** 1–24.

Castle ES. 1942. Spiral growth and reversal of spiraling in *Phycomyces*, and their bearing on primary wall structure. *American Journal of Botany* **29,** 664–672.

Castle ES. 1958. The topography of tip growth in a plant cell. *Journal of General Physiology* **41,** 913–926.

Chung S, Shin SH, De Yoreo JJ, Bertozzi CR. 2010. Self-catalyzed growth of S-layer via amorphous-to-crystalline transition limited by folding kinetics. *Proceedings of the National Academy of Sciences, USA* **107,** 16536–16541.

Cleland R. 1971. The mechanical behavior of isolated *Avena* coleoptile walls subjected to constant stress. Properties and relation to cell elongation. *Plant Physiology* **47,** 805–811.

Cormack RGH. 1949. The development of root hairs in angiosperms. *Botanical Reviews* **15,** 583–612.

Cormack RGH. 1954. On the growth of root hairs. *Science* **119,** 615–616.

Cosgrove DJ. 1997. Assembly and enlargement of the primary cell wall in plants. *Annual Review of Cell and Developmental Biology* **13,** 171–201.

Cosgrove DJ. 2000. Loosening of plant cell walls by expansins. *Nature* **407,** 321–326.

Cosgrove DJ. 2005. Growth of the plant cell wall. *Nature Reviews* **6,** 850–861.

Couturier E, Dumais J, Cerda E, Katifori E. 2013. Folding of an opened spherical shell. *Soft Matter* doi: 10.1039/C3SM50575H [Epub ahead of print].

Crick FHC, Watson JD. 1956. Structure of small viruses. *Nature* **177,** 473–475.

Dombrowski C, Kan W, Motaleb MdA, Charon NW, Goldstein RE, Wolgemuth CW. 2009. The elastic basis for the shape of *Borrelia burgdorferi*. *Biophysical Journal* **96,** 4409–4417.

Domínguez-Escobar J, Chastanet A, Crevenna AH, Fromion V, Wedlich-Söldner R, Carballido-López R. 2011. Processive movement of MreB-associated cell wall biosynthetic complexes in bacteria. *Science* **333,** 225–228.

Dumais J, Long SR, Shaw SL. 2004. The mechanics of surface expansion anisotropy in *Medicago truncatula* root hairs. *Plant Physiology* **136,** 3266–3275.

Dumais J, Shaw SL, Steele CR, Long SR, Ray PM. 2006. An anisotropic–viscoplastic model of plant cell morphogenesis by tip growth. *International Journal of Developmental Biology* **50,** 209–222.

Elgsaeter A, Stokke BT, Mikkelsen A, Branton D. 1986. The molecular basis of erythrocyte shape. *Science* **234,** 1217–1223.

Franks PJ, Cowan IR, Farquhar GD. 1998. A study of stomatal mechanics using the cell pressure probe. *Plant, Cell & Environment* **21,** 94–100.

Fry SC. 2004. Primary cell wall metabolism: tracking the careers of wall polymers in living plant cells. *New Phytologist* **161,** 641–675.

Fry SC, **Smith RC**, **Renwick KF**, **Martin DJ**, **Hodge SK**, **Matthews KJ**. 1992. Xyloglucan endotransglycosylase, a new wall-loosening enzyme activity from plants. *Biochemical Journal* **282,** 821–828.

Garner EC, Bernard R, Wang W, Zhuang X, Rudner DZ, Mitchison T. 2011. Coupled, circumferential motions of the cell wall synthesis machinery and MreB filaments in *B. subtilis*. *Science* **333,** 222–225.

Geitmann A, Ortega JKE. 2009. Mechanics and modeling of plant cell growth. *Trends in Plant Sciences* **14,** 467–478

Green PB, Erickson RO, Richmond PA. 1970. On the physical basis of cell morphogenesis. *Annals of the New York Academy of Sciences* **175,** 712–731.

Green PB. 1954. The spiral growth pattern of the cell wall in *Nitella axillaris*. *American Journal of Botany* **41,** 403–409.

Green PB. 1969. Cell morphogenesis. *Annual Reviews of Plant Physiology* **20,** 365–394.

Halbritter HM, Hesse M. 2004. Principal modes of infoldings in tricolp(or)ate angiosperm pollen. *Grana* **43,** 1–14.

Harold FM. 1990. To shape a cell: an inquiry into the causes of morphogenesis of microorganisms. *Microbiological Reviews* **54,** 381–431.

Harris WF. 1970. Topological restrictions on the distribution of defects in surface crystals and possible biophysical applications. In: Simmons JA, deWit R, Bullough R, eds. *Fundamental aspects of dislocation theory* . Special Publication No. 317, Vol. **1**. Washington, DC: National Bureau of Standards, 579–592.

Harris WF, Scriven LE. 1970. Function of dislocations in cell walls and membranes. *Nature* **228,** 827–829.

Harris WF, Scriven LE. 1971. Intrinsic disclinations as dislocations sources and sinks in surface crystals. *Journal of Applied Physics* **42,** 3309–3312.

Haughton PM, Sellen DB. 1969. Dynamic mechanical properties of the cell wall of some green algae. *Journal of Experimental Botany* **20,** 516–535.

Hejnowicz Z, Heinemann B, Sievers A. 1977. Tip growth: patterns of growth rate and stress in the *Chara* rhizoid. *Zeitschrift für Pflanzenphysiologie* **81,** 409–424.

Henriksen K, Stipp SLS, Young JR, Marsh ME. 2004. Biological control on calcite crystallisation: AFM investigation of coccolith polysaccharide function. *American Mineralogist* **89,** 1709–1716.

Henriksen K, Stipp SLS. 2009. Controlling biomineralization: the effect of solution composition on coccolith polysaccharide functionality. *Crystal Growth Design* **9,** 2088–2097.

Heslop-Harrison J. 1979a. An interpretation of the hydrodynamics of pollen. *American Journal of Botany* **66,** 737–743.

Heslop-Harrison J. 1979b. Pollen walls as adaptive systems. *Annals of the Missouri Botanical Garden* **66,** 813–829.

Höltje JV. 1998. Growth of the stress-bearing and shape-maintaining murein sacculus of *Escherichia coli*. *Microbiology and Molecular Biology Reviews* **62,** 181–203.

Houwink AL. 1956. Flagella, gas vacuoles and cell-wall structure in *Halobacterium halobium*; an electron microscopy study. *Journal of General Biology* **15,** 146–150.

Hovenkamp PH, Van Der Ham RWJM, Van Uffelen GA, Van Hecke M, Dijksman JA, Star W. 2009. Spore movement driven by the spore wall in an eusporangiate fern. *Grana* **48,** 122–127

Howard LV, Dalton DD, McCoubrey WK Jr. 1982. Expansion of the tetragonally arrayed cell wall protein layer during growth of *Bacillus sphaericus*. *Journal of Bacteriology* **149,** 748–757.

Katifori I, Alben S, Cerda E, Nelson DR, Dumais J. 2010. Foldable structures and the natural design of pollen grains. *Proceedings of the National Academy of Sciences, USA* **107,** 7635–7639.

Landau LD, Lifshitz EM. 1986. *Theory of elasticity* . Oxford: Pergamon Press.

Leedale GF. 1964. Pellicle structure in *Euglena*. *British Phycological Bulletin* **2,** 291–306.

Leedale GF, Meeuse BJD, Pringsheim EG. 1965. Structure and physiology of *Euglena spirogyra*. I and II. *Archiv für Mikrobiologie* **50,** 68–102.

Marsh ME. 2003. Regulation of $CaCO_3$ formation in coccolithophores. *Comparative Biochemistry and Physiology B* **136,** 743–754.

Messner P, Pum D, Sára M, Stetter K O, Sleytr UB. 1986. Ultrastructure of the cell envelope of the archaebacteria *Thermoproteus tenax* and *Thermoproteus neutrophilus*. *Journal of Bacteriology* **166,** 1046–1054.

Noblin X, Rojas N, Westbrook J, Llorens C, Argentina M, Dumais J. 2012. The fern sporangium: a unique catapult. *Science* **335,** 1322.

Peaucelle A, Braybrook S, Hofte H. 2012. Cell wall mechanics and growth control in plants: the role of pectins revisited. *Frontiers in Plant Sciences* **3,** 121.

Pickett-Heaps J, Schmid AMM, Edgar LA. 1990. The cell biology of diatom valve formation. *Progress in Phycological Research* **7,** 1–168.

Pogorelov AV. 1988. *Bending of surfaces and stability of shells*. Providence, RI: American Mathematical Society.

Proseus TE, Boyer JS. 2006. Calcium pectate chemistry controls growth rate of *Chara corallina*. *Journal of Experimental Botany* **57,** 3989–4002.

Proseus TE, Zhu GL, Boyer JS. 2000. Turgor, temperature and the growth of plant cells: using *Chara corallina* as a model system. *Journal of Experimental Botany* **51,** 1481–1494.

Pum D, Messner P, Sleytr UB. 1991. Role of the S layer in morphogenesis and cell division of the archaebacterium *Mathenocorpusculum sinense*. *Journal of Bacteriology* **173,** 6865–6873.

Ray PM. 1987. Principles of plant cell expansion. In: Cosgrove DJ, Knievel DP, eds, *Physiology of cell expansion during plant growth* . Rockville, MD: American Society of Plant Physiologists, 1–17.

Ray PM. 1992. Mechanisms of wall loosening for cell growth. *Current Topics in Plant Biochemistry and Physiology* **11,** 18–41.

Ray PM, Ruesink AW. 1962. Kinetic experiments on the nature of the growth mechanism in oat coleoptile cells. *Developmental Biology* **4,** 377–397.

Roberts K, Grief C, Hills GJ, Shaw PJ. 1985. Cell wall glycoproteins: structure and function. *Journal of Cell Science Supplement* **2,** 105–127.

Rojas ER, Hotton S, Dumais J. 2011. Chemically-mediated mechanical expansion of the pollen tube cell wall. *Biophysical Journal* **101,** 1844–1853.

Schols HK, Voragen AGJ. 2002. The chemical structure of pectins. In: Seymour GP, Knox JP, eds. *Pectins and their manipulation* . Oxford: Blackwell Publishing/CRC Press, 1–29.

Shaw SL, Dumais J, Long SR. 2000. Cell surface expansion in polarly growing root hairs of *Medicago truncatula*. *Plant Physiology* **124,** 959–969.

Sheetz MP, Singer SJ. 1974. Biological membranes as bilayer couples. A molecular mechanism of drug-erythrocyte interactions. *Proceedings of the National Academy of Sciences, USA* **71,** 4457–4461.

Sliusarenko O, Cabeen MT, Wolgemuth CW, Jacobs-Wagner C, Emonet T. 2010. Processivity of peptidoglycan synthesis provides a built-in mechanism for the robustness of straight-rod cell morphology. *Proceedings of the National Academy of Sciences, USA* **107,** 10086–10091

Spero HJ. 1988. Ultrastructural examination of chamber morphogenesis and biomineralization in the planktonic foraminifer *Orbulina universa*. *Marine Biology* **99,** 9–20.

Suzaki T, Williamson RE. 1985. Euglenoid movement in *Euglena fusca*: evidence for sliding between pellicular strips. *Protoplasma* **124,** 137–146.

Suzaki T, Williamson RE. 1986. Cell surface displacement during euglenoid movement and its computer simulation. *Cell Motility and the Cytoskeleton* **6,** 186–192.

Thompson DW. 1942. *On growth and form* . Cambridge: Cambridge University Press.

Trachtenberg S, Gilad R, Geffen N. 2003. The bacterial linear motor of *Spiroplasma melliferum* BC3: from single molecules to swimming cells. *Molecular Microbiology* **47,** 671–697.

Vesque J. 1883. Sur l'organization mécanique du grain de pollen. *Comptes Rendus de l'Académie des Sciences* **96,** 1684–1686.

Vollmer W, Bertsche U. 2008. Murein (peptidoglycan) structure, architecture and biosynthesis in *Escherichia coli*. *Biochimica et Biophysica Acta* **1778,** 1714–1734.

Wang P, Robert L, Pelletier J, Dang WL, Taddei F, Wright A, Jun S. 2010. Robust growth of *Escherichia coli*. *Current Biology* **20,** 1099–1103.

Wang S, Furchtgott L, Huang KC, Shaevitz JW. 2012. Helical insertion of peptidoglycan produces chiral ordering of the bacterial cell wall. *Proceedings of the National Academy of Sciences, USA* **109,** E595–E604.

Wodehouse RP. 1935. *Pollen grains* . New York: McGraw-Hill.

Woessner JP, Goodenough UW. 1994. Volvocine cell walls and their constituent glycoproteins: an evolutionary perspective. *Protoplasma* **181,** 245–258.

Wold MP, Gamow RI. 1992. Fiber composite model for helical growth in the *Phycomyces* cell wall. *Journal of Theoretical Biology* **159,** 39–51.

Wolgemuth CW, Inclan YF, Quan J, Mukherjee S, Oster G, Koehl MAR. 2005. How to make a spiral bacterium. *Physical Biology* **2,** 189–199.